LETTER

doi:10.1038/nature12670

Decoupling of soil nutrient cycles as a function of aridity in global drylands

Manuel Delgado-Baquerizo[1,2], Fernando T. Maestre[2], Antonio Gallardo[1], Matthew A. Bowker[3], Matthew D. Wallenstein[4], Jose Luis Quero[2,5], Victoria Ochoa[2], Beatriz Gozalo[2], Miguel García-Gómez[2], Santiago Soliveres[2], Pablo García-Palacios[4,6], Miguel Berdugo[2], Enrique Valencia[2], Cristina Escolar[2], Tulio Arredondo[7], Claudia Barraza-Zepeda[8], Donaldo Bran[9], José Antonio Carreira[10], Mohamed Chaieb[11], Abel A. Conceição[12], Mchich Derak[13], David J. Eldridge[14], Adrián Escudero[2], Carlos I. Espinosa[15], Juan Gaitán[9], M. Gabriel Gatica[16], Susana Gómez-González[17], Elizabeth Guzman[15], Julio R. Gutiérrez[8], Adriana Florentino[18], Estela Hepper[19], Rosa M. Hernández[20], Elisabeth Huber-Sannwald[7], Mohammad Jankju[21], Jushan Liu[22], Rebecca L. Mau[23], Maria Miriti[24], Jorge Monerris[25], Kamal Naseri[21], Zouhaier Noumi[11], Vicente Polo[2], Aníbal Prina[19], Eduardo Pucheta[16], Elizabeth Ramírez[20], David A. Ramírez-Collantes[26], Roberto Romão[12], Matthew Tighe[27], Duilio Torres[28], Cristian Torres-Díaz[17], Eugene D. Ungar[29], James Val[30], Wanyoike Wamiti[31], Deli Wang[22] & Eli Zaady[32]

The biogeochemical cycles of carbon (C), nitrogen (N) and phosphorus (P) are interlinked by primary production, respiration and decomposition in terrestrial ecosystems[1]. It has been suggested that the C, N and P cycles could become uncoupled under rapid climate change because of the different degrees of control exerted on the supply of these elements by biological and geochemical processes[1–5]. Climatic controls on biogeochemical cycles are particularly relevant in arid, semi-arid and dry sub-humid ecosystems (drylands) because their biological activity is mainly driven by water availability[6–8]. The increase in aridity predicted for the twenty-first century in many drylands worldwide[9–11] may therefore threaten the balance between these cycles, differentially affecting the availability of essential nutrients[12–14]. Here we evaluate how aridity affects the balance between C, N and P in soils collected from 224 dryland sites from all continents except Antarctica. We find a negative effect of aridity on the concentration of soil organic C and total N, but a positive effect on the concentration of inorganic P. Aridity is negatively related to plant cover, which may favour the dominance of physical processes such as rock weathering, a major source of P to ecosystems, over biological processes that provide more C and N, such as litter decomposition[12–14]. Our findings suggest that any predicted increase in aridity with climate change will probably reduce the concentrations of N and C in global drylands, but increase that of P. These changes would uncouple the C, N and P cycles in drylands and could negatively affect the provision of key services provided by these ecosystems.

Biogeochemical cycles are biologically coupled, on molecular to global scales, owing to the conserved elemental stoichiometry of plants and microorganisms that drive the cycling of C, N and P (ref. 1). The availability of C and N is primarily linked to biological processes such as photosynthesis, atmospheric N fixation and subsequent microbial mineralization[12–14]. However, available P for plants and microorganisms[2,13,14] is derived mainly from mechanical rock weathering and, to a lesser extent, from the decomposition of organic matter[12–14]. The importance of biological control of nutrient cycling relative to geochemical control has been shown to change with ecosystem development[2,13,14]. For example, during the earliest stages of ecosystem succession, a relative prevalence of geochemical control on nutrient cycling means that P is made available by mechanical rock weathering, but that N and C are scarce, leading to a disparity in the C, N and P cycles relative to plant nutrient requirements[13–16]. Climatic controls on ecosystem development and biogeochemical cycles are particularly relevant in drylands because their biological activity is mainly driven by water availability[6–8]. Drylands cover about 41% of Earth's land surface and support more than 38% of the global human population[17], constituting the largest terrestrial biome on the planet[18]. The increase in aridity predicted for the late-twenty-first century in many regions worldwide will increase the total area of drylands globally[9–11]. These changes are predicted to exacerbate processes leading to land degradation and desertification, which already threaten the livelihood of more than 250 million people living in drylands[17,18]. For example, a worldwide decrease in soil moisture by 5–15% has been predicted for the 2080–2099 period[11]. Of particular concern is that the

[1]Departamento de Sistemas Físicos, Químicos y Naturales, Universidad Pablo de Olavide, Carretera de Utrera, kilómetro 1, 41013 Sevilla, Spain. [2]Area de Biodiversidad y Conservación, Departamento de Biología y Geología, Escuela Superior de Ciencias Experimentales y Tecnología, Universidad Rey Juan Carlos, Calle Tulipán Sin Número, 28933 Móstoles, Spain. [3]School of Forestry, Northern Arizona University, Flagstaff, Arizona 86011, USA. [4]Natural Resource Ecology Laboratory, Colorado State University, Fort Collins, Colorado 80523, USA. [5]Departamento de Ingeniería Forestal, Campus de Rabanales Universidad de Córdoba, Carretera de Madrid, kilómetro 396, 14071 Córdoba, Spain. [6]Department of Biology, Colorado State University, Fort Collins, Colorado 80523, USA. [7]División de Ciencias Ambientales, Instituto Potosino de Investigación Científica y Tecnológica, San Luis Potosí, San Luis Potosí, 78210, Mexico. [8]Departamento de Biología, Universidad de La Serena, La Serena 599, 1700000, Chile. [9]Instituto Nacional de Tecnología Agropecuaria, Estación Experimental San Carlos de Bariloche 277, Bariloche, Río Negro, 8400, Argentina. [10]Universidad de Jaen, Departamento de Biología Animal, Biología Vegetal y Ecología, 23071 Jaen, Spain. [11]Université de Sfax, Faculté des Sciences, Unité de Recherche Plant Diversity and Ecosystems in Arid Environments, Route de Sokra, kilomètre 3.5, Boîte Postale 802, 3018 Sfax, Tunisia. [12]Departamento de Ciências Biológicas, Universidade Estadual de Feira de Santana, Avenida Transnordestina Sin Número, Bairro Novo Horizonte, Feira de Santana, 44036-900, Brasil. [13]Direction Régionale des Eaux et Forêts et de la Lutte Contre la Désertification du Rif, Avenue Mohamed 5, Boîte Postale 722, 93000 Tétouan, Morocco. [14]School of Biological, Earth and Environmental Sciences, University of New South Wales, Sydney, New South Wales 2052, Australia. [15]Instituto de Ecología, Universidad Técnica Particular de Loja, San Cayetano Alto, Marcelino Champagnat, Loja, 11-01-608, Ecuador. [16]Departamento de Biología, Facultad de Ciencias Exactas, Físicas y Naturales, Universidad Nacional de San Juan, Rivadavia, San Juan, J5402DCS, Argentina. [17]Laboratorio de Genómica y Biodiversidad, Departamento de Ciencias Básicas, Universidad del Bío-Bío 447, Chillán, 3780000, Chile. [18]Instituto de Edafología, Facultad de Agronomía, Universidad Central de Venezuela, Ciudad Universitaria, Caracas, 1051, Venezuela. [19]Facultad de Agronomía, Universidad Nacional de La Pampa, Casilla de Correo 300, 6300 Santa Rosa, La Pampa, Argentina. [20]Laboratorio de Biogeoquímica, Centro de Agroecología Tropical, Universidad Experimental Simón Rodríguez, Caracas, 47925, Venezuela. [21]Department of Range and Watershed Management, Faculty of Natural Resources and Environment, Ferdowsi University of Mashhad, Azadi Square, Mashhad 91775–1363, Iran. [22]Institute of Grassland Science, Northeast Normal University and Key Laboratory of Vegetation Ecology, Ministry of Education, Changchun, Jilin Province 130024, China. [23]Department of Biological Sciences, Northern Arizona University, PO Box 5640, Flagstaff, Arizona 86011–5640, USA. [24]Department of Evolution, Ecology and Organismal Biology, Ohio State University, 318 West 12th Avenue, Columbus, Ohio 43210, USA. [25]Université du Québec à Montréal Pavillon des Sciences Biologiques, Département des Sciences Biologiques, 141 Président-Kennedy, Montréal, Québec H2X 3Y5, Canada. [26]Production Systems and the Environment Sub-Program, International Potato Center. Apartado 1558, Lima 12, Peru. [27]Department of Agronomy and Soil Science, School of Environmental and Rural Science, University of New England, Armidale, New South Wales 2351, Australia. [28]Departamento de Química y Suelos, Decanato de Agronomía, Universidad Centroccidental "Lisandro Alvarado", Barquisimeto 3001, Venezuela. [29]Department of Agronomy and Natural Resources, Institute of Plant Sciences, Agricultural Research Organization, The Volcani Center, Bet Dagan 50250, Israel. [30]Office of Environment and Heritage, PO Box 363, Buronga, New South Wales 2739, Australia. [31]Zoology Department, National Museums of Kenya, Ngara Road, Nairobi, 78420-00500, Kenya. [32]Department of Natural Resources and Agronomy, Agriculture Research Organization, Ministry of Agriculture, Gilat Research Center, Mobile Post Negev 85280, Israel.

biogeochemical cycles of C, N and P could become uncoupled under rapid climate change because of the different degrees of control exerted on these elements by biological and geochemical processes[1–5]. As the global human population continues to grow, we will rely increasingly on marginal lands—particularly drylands—for the production of food, wood and biofuels, and to offset the emission of greenhouse gases[3,4,17,18]. These ecosystem services can be greatly and negatively affected by the decoupling of the biogeochemical cycles of C, N and P in soils[3,4,17,18]. Despite the importance of these cycles for ecosystem functioning and human welfare, it is largely unknown how predicted increases in aridity may influence them[4,18], and no global field studies have yet been conducted on this topic[19].

We evaluated how aridity affects the balance between C, N and P in soils collected from 224 dryland sites from all continents except Antarctica. Because aridity is a fundamental driver of biological and geochemical processes in drylands[8,12,17], we predicted that increasing aridity would reduce biological activity[4,5] and, therefore, the availability in nutrients under more strict biological control[3] (C and N), but would favour the relative dominance of nutrients linked to geochemical processes[1–4,13,20] (P), causing a stoichiometric imbalance in the nutrient cycles associated with C and N (ref. 3). We selected organic C, total N and total P as surrogates for C, N and P availability because they were highly related to other available C, N and P forms for plants and microorganisms such as dissolved carbohydrates, amino acids, inorganic N, Olsen inorganic P and HCl-P (fraction of P linked to calcium carbonate minerals) (Methods). Negative quadratic relationships were observed between aridity and both organic C and total N concentrations (Fig. 1a, c). Although nonsignificant, a positive trend was observed between aridity and total P (Fig. 1e). This relationship was significant when inorganic P was considered instead of total P (Extended Data Fig. 1a). Likewise, a negative quadratic relationship was observed between aridity and the N:P and C:P concentration ratios (Fig. 1b, d and Extended Data Fig. 1b, c). The C:N ratio decreased linearly with increasing aridity (Fig. 1f). Similar results were found when evaluating relationships between aridity and more labile C (carbohydrates), N (sum of dissolved inorganic N and amino acids) and P (available P) fractions, as well as with their respective C, N and P ratios (Extended Data Fig. 2). Mechanical rock weathering is the main P input into terrestrial ecosystems, but N is either absent from or uncommon in primary minerals, and inputs therefore are largely derived from atmospheric N fixation, deposition or both[13,14]. Although rates of biological weathering should decrease with increasing aridity, mechanical rock weathering may increase with aridity, releasing P-bearing

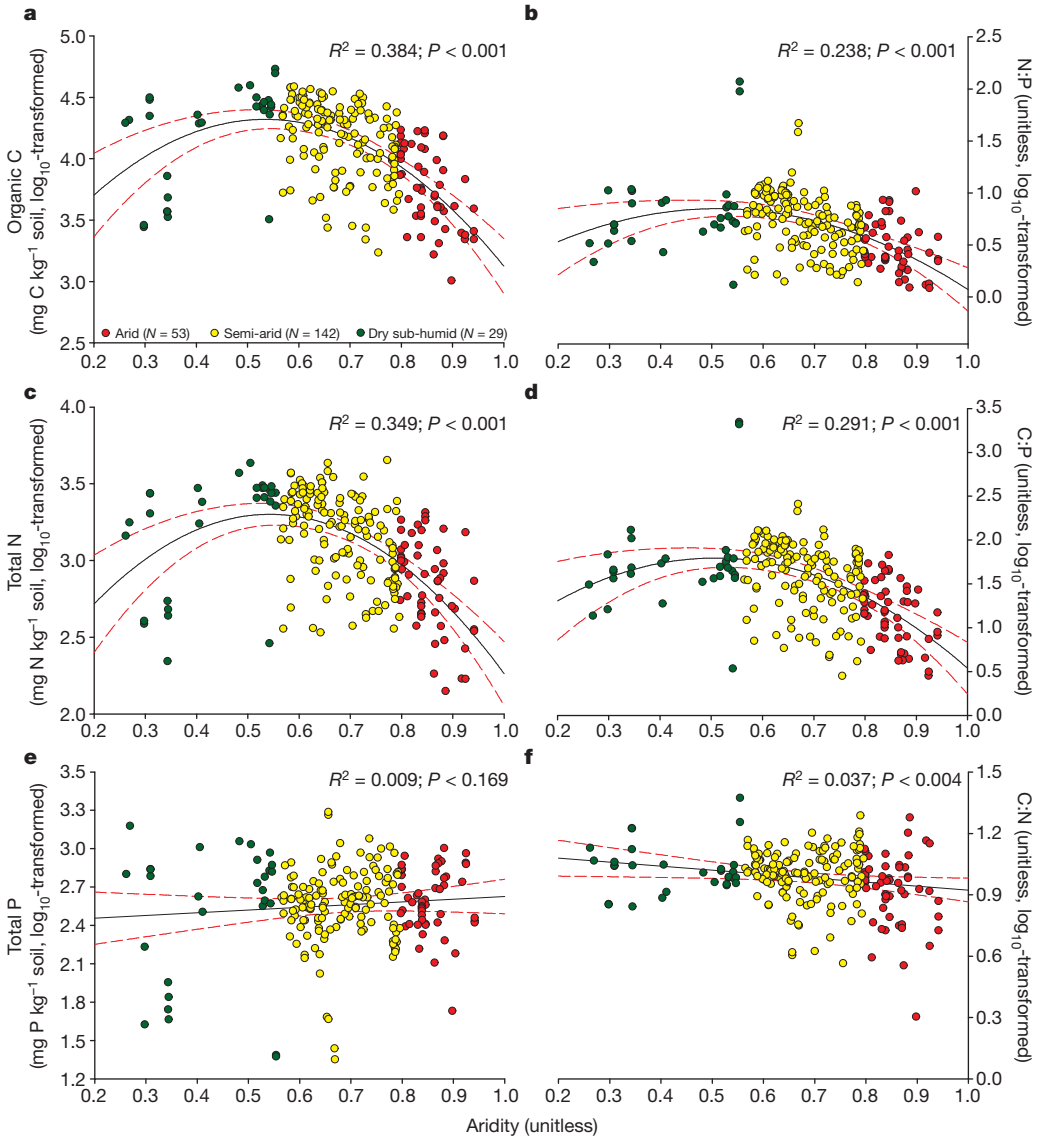

Figure 1 | Relationships between aridity and C, N and P at our study sites. **a**, Organic C; **b**, N:P; **c**, total N; **d**, C:P; **e**, total P; **f**, C:N. Aridity is defined as 1 – AI, where AI, the ratio of precipitation to potential evapotranspiration, is the aridity index. The solid and dashed lines represent the fitted quadratic regressions and their 95% confidence intervals, respectively. R^2, proportion of variance explained.

minerals[14,18,21]. Furthermore, the reduced plant activity and nutrient uptake typically observed in the most arid sites can also promote a higher availability of P at these sites[2,7,12,14]. In addition, we found a positive relationship between aridity and the concentration of HCl-P (Extended Data Fig. 3). These results suggest that at least part of the increase in P derived from increasing aridity may be associated with the calcium carbonate minerals. High concentrations of calcium carbonates are likely to occur in the most arid soils because the low rainfall and high evaporation prevent weathering products from being washed out of the soil profile[20].

To clarify the effects and relative importance of aridity on the availability of C, N and P, we generated a structural equation model based on the known effects and relationships between key drivers of organic C, total N and total P (Extended Data Fig. 4). We included in this model phosphatase activity, which is the enzyme responsible for releasing inorganic P from organic sources and is considered a surrogate of biological P demand[15,22,23]. Our model explained 43%, 26% and 53% of the variance in the organic matter component (first component from a principal-component analysis (PCA) conducted with organic C and total N), total P and phosphatase activity, respectively. Aridity had a direct negative effect on the organic matter component and phosphatase activity, but a positive effect on total P (Fig. 2). In addition, aridity was also the most important predictor of the organic matter component and phosphatase activity (Fig. 3). Similar results were found when we used inorganic P instead of total P in this model (Extended Data Figs 5 and 6) and when we included a more labile organic matter component (first component from a PCA with carbohydrates and available N) and available P (Extended Data Figs 7 and 8).

Our results imply a set of predictions. Forecasted increases in aridity in drylands globally[9–11] are expected to lead to severe nutrient depletion[14] in these environments, particularly in the most arid sites. For example, the observed decrease in N in drylands with increasing aridity (probably derived from the higher soil erosion and the lower plant cover), which

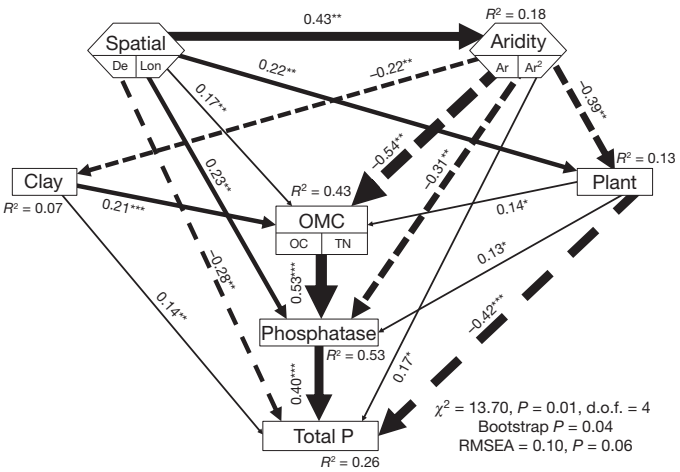

Figure 2 | Effects of aridity, clay percentage, plant cover and site position on the organic matter component, total-P concentration and phosphatase activity. Spatial coordinates of the study sites are expressed in terms of distance from Equator (De) and longitude (Lon). Numbers adjacent to arrows are standardized path coefficients, analogous to relative regression weights, and indicative of the effect size of the relationship. Continuous and dashed arrows indicate positive and negative relationships, respectively. Arrow width is proportional to the strength of the relationship. The proportion of variance explained (R^2) appears alongside every response variable in the model. Goodness-of-fit statistics for each model are shown in the lower right corner (d.o.f., degrees of freedom; RMSEA, root mean squared error of approximation). There are some differences between the a-priori model and the final model structures, owing to removal of paths with coefficients close to zero (see the a-priori model in Extended Data Fig. 4). Hexagons are composite variables[30]. Squares are observable variables. The organic matter component (OMC) is the first component from a PCA conducted with soil organic carbon (OC) and total nitrogen (TN). $*P < 0.05$, $**P < 0.01$, $***P < 0.001$.

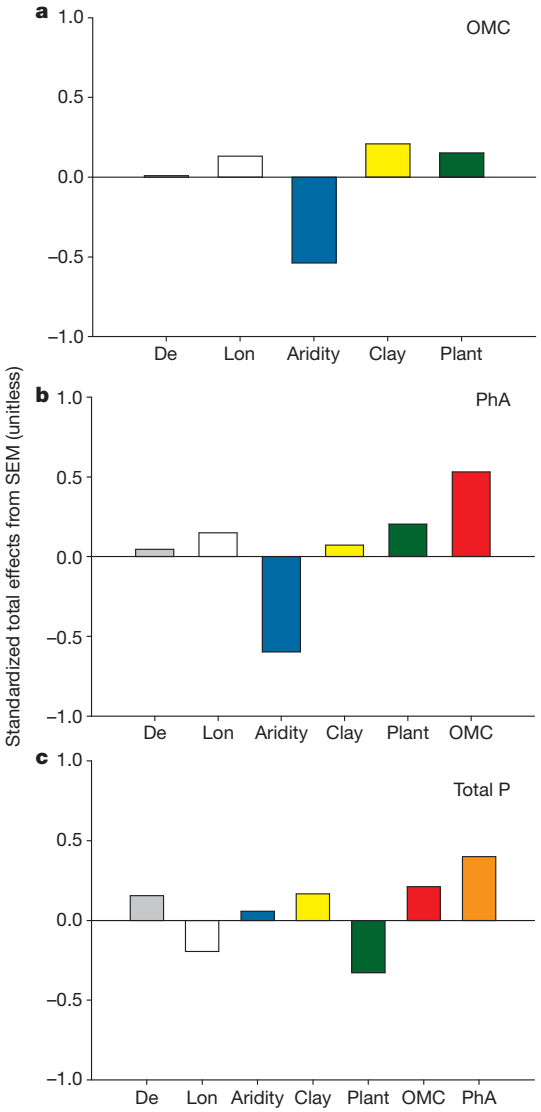

Figure 3 | Standardized total effects (direct plus indirect effects) derived from the structural equation modelling. These include the effects of aridity, percentage of clay, plant cover, distance from Equator (De) and longitude (Lon) on the organic matter component (OMC; first component from a PCA conducted with soil organic C and total N), total P and phosphatase activity (PhA). SEM, structural equation model.

are already poor in nutrients[4,12], could inhibit N mineralization in soils, potentially leading to a positive feedback on nutrient availability[24] (Extended Data Figs 9 and 10). The observed increase in the N:P ratio with decreasing aridity is similar to what would be expected during long-term ecosystem development[13,14]. Although this progression has been described on the geological timescale (thousands to millions of years), and changes in aridity occur on the ecological timescale (tens to thousands of years), the processes may share the same biogeochemical signatures, such as N and P accumulation mediated by shifts in the relative importance of biological and geochemical processes[13,14]. Thus, in the more arid sites, inorganic P accumulates by geochemical weathering because of the low net primary production and nutrient plant uptake characterizing these ecosystems, and is associated with calcium carbonate minerals. However, N is only slowly incorporated by N fixation[13,14], being also limited by low C (energy) availability[1,3]. In the less arid sites (dry sub-humid ecosystems), where N and C are already available for plants and microorganisms, P becomes available through the activity of extracellular phosphatase enzymes[14] (which require N investment), coupling P availability to biological processes[24].

Predicted increases in aridity, and, hence, decreases in water availability, are also expected to reduce plant cover in drylands[5] (Fig. 2), favouring the dominance of physical processes[21] (for example the abrasion of exposed rock surfaces by wind-blown sands) over biological processes (for example litter decomposition and N fixation), decreasing the concentration of N and C (for example because of the wind erosion) and increasing the concentration of P (for example because of bedrock rejuvenation) in soils, hence distorting soil C, N and P cycles[1,21]. Carbon and N become uncoupled from P in response to increasing aridity (Fig. 1). Under arid and semi-arid conditions, the reduced availability of C and N may unbalance the concentrations of C, N and P, constraining plant and microbial activity and diversity[1,3]. This may have an important negative effect on primary production and organic matter decomposition[1,18,24], even when P is available. In addition, the observed decrease in phosphatase activity and the increase in P observed in coarser, sandier soils with increasing aridity suggests that key abiotic and biotic processes, such as soil formation and organic matter decomposition, may be reduced with increasing aridity[21]. The decrease in the C:N ratio with increasing aridity observed here accords with experimental studies showing that drought periods decouple C and N cycles in drylands[25]. Although organic C and total N are strongly correlated in the studied sites (Pearson's $r = 0.92$), our results suggest that future climatic conditions will promote N losses in drylands, particularly if increases in aridity reduce vegetation cover in these ecosystems (Fig. 2). The imbalance observed in the C, N and P cycles with increasing aridity may have other important consequences for drylands. For example, reductions in N availability as a consequence of increases in aridity will limit the capacity of plant primary productivity to buffer human-induced increases in atmospheric CO_2 concentrations, because the rate of photosynthesis is proportional to the amount and activity of the N-rich enzyme ribulose bisphosphate carboxylase/oxygenase in leaves[1,25]. This would contribute to a warmer world by the end of the twenty-first century, by limiting the capacity of plants and microorganisms to fix CO_2 derived from human activities[1,3,26]. In addition, decreases in the supply of N relative to that of P may have a short-term effect by differentially constraining the growth rates of plant species based on their stoichiometry[3]. Such reductions may also have long-term evolutionary effects by selecting plants and microorganisms with different levels of N in their nucleotides, potentially altering ecosystem structural and functional traits[3].

Our results indicate that the coupling between biogeochemical cycles in drylands will be particularly fragile in the face of rapid climate change, especially in the areas of transition between semi-arid and arid climates. Carbon, N and P availability seemed to be more resistant to changes in aridity in the transition from dry sub-humid to semi-arid climates than from semi-arid to arid, where we observed substantial and abrupt declines in organic C and total N, but an increase in inorganic P (Fig. 1a, c; Extended Data Fig. 1a). Similarly, we observed an abrupt decrease in the N:P and C:P ratios between semi-arid and arid sites, which was not observed in the C:N ratio (Fig. 1b, d, f). Evaluation of critical global transitions and tipping points is of major importance in assessing the effects of global change on ecosystems, and is an area of active research[27]. The abrupt changes observed in the C:P and N:P ratios in the transitions from semi-arid to arid climates, together with the predicted increase in the proportion of global drylands considered to be arid[9], may force these systems into a long process towards the recovery of ecosystem stoichiometry.

Our findings suggest that the predicted increase in aridity across drylands worldwide will reduce the concentration of biologically controlled C and N, but will increase that of P, which is primarily derived from rock weathering. These changes are likely to interrupt the C, N and P cycles in drylands in a nonlinear manner, and will have negative effects on biogeochemical reactions controlling key ecosystem functions (for example primary production, respiration and decomposition) and services (for example food production and carbon storage) from local to global scales[1].

METHODS SUMMARY

Field data were collected from 224 dryland sites located in 16 countries from all continents except Antarctica. At each site, to measure the total cover of perennial plants we established a 30 m × 30 m plot representative of the dominant vegetation[28]. Five composite samples (0–7.5-cm depth) were randomly taken under the canopy of the dominant perennial plant species and in open areas devoid of perennial vegetation. The percentage of perennial plant cover; the percentage of clay; the concentrations of organic C, total N and total P; and the activity of phosphatase were determined as described in ref. 28. All these variables were then averaged to obtain site-level estimates by using the mean values observed in bare ground and vegetated areas, weighted by their respective cover at each site.

We first explored the relationship between aridity and organic C, total N, total P and the N:P, C:P and N:C ratios by using either linear or curvilinear regressions. We estimated the aridity[19] (1 – AI) of each site using data from the WorldClim global database[29]. We then used structural equation modelling[30] to examine the relative importance of aridity for organic C, total N, total P and phosphatase activity. Because organic C and total N were very closely related (Pearson's $r = 0.92$), we reduced these two variables to a single variable using PCA of the correlation matrix. We then introduced the first component of this PCA as a new variable into the model (organic matter component).

We evaluated the fit of our model using the model χ^2-test and the root mean squared error of approximation; because the residuals of some data were not normally distributed, we confirmed fit using the Bollen–Stine bootstrap test (Fig. 2).

Online Content Any additional Methods, Extended Data display items and Source Data are available in the online version of the paper; references unique to these sections appear only in the online paper.

Received 19 March; accepted 17 September 2013.

1. Finzi, A. C. *et al.* Coupled biochemical cycles: responses and feedbacks of coupled biogeochemical cycles to climate change. Examples from terrestrial ecosystems. *Front. Ecol. Environ* **9,** 61–67 (2011).
2. McGill, W. B. & Cole, C. V. Comparative aspects of cycling organic C, N, S and P through soil organic matter. *Geoderma* **26,** 267–286 (1981).
3. Peñuelas, J. *et al.* The human-induced imbalance between C, N and P in Earth's life system. *Glob. Change Biol.* **18,** 3–6 (2012).
4. Schlesinger, W. H. *et al.* Biological feedbacks in global desertification. *Science* **247,** 1043–1048 (1990).
5. Vicente-Serrano, S. M. *et al.* Dryness is accelerating degradation of vulnerable shrublands in semiarid Mediterranean environments. *Ecol. Monogr.* **82,** 407–428 (2012).
6. Austin, A. T. *et al.* Water pulses and biogeochemical cycles in arid and semiarid ecosystems. *Oecologia* **141,** 221–235 (2004).
7. Schwinning, S. & Sala, O. E. Hierarchy of responses to resource pulses in arid and semi-arid ecosystems. *Oecologia* **141,** 211–220 (2004).
8. Whitford, W. G. *Ecology of Desert Systems* (Academic, 2002).
9. Gao, X. J. & Giorgi, F. Increased aridity in the Mediterranean region under greenhouse gas forcing estimated from high resolution simulations with a regional climate model. *Global Planet. Change* **62,** 195–209 (2008).
10. Feng, S. & Fu, Q. Expansion of global drylands under a warming climate. *Atmos. Chem. Phys. Discuss.* **13,** 14637–14665 (2013).
11. Dai, A. Increasing drought under global warming in observations and models. *Nature Clim. Change* **3,** 52–58 (2013).
12. Schlesinger, W. H. *Biogeochemistry, an Analysis of Global Change* (Academic, 1996).
13. Walker, T. W. & Syers, J. K. The fate of phosphorus during pedogenesis. *Geoderma* **15,** 1–19 (1976).
14. Vitousek, P. M. *Nutrient Cycling and Limitation: Hawai'i as a Model System* (Princeton Univ. Press, 2004).
15. Nannipieri, P. *et al. Phosphorus in Action* (Soil Biol. 26, Springer, 2011).
16. Liebig, J. *et al. Chemistry in its Application to Agriculture and Physiology* 3rd edn (Owen, 1842).
17. Reynolds, J. F. *et al.* Global desertification: building a science for dryland development. *Science* **316,** 847–851 (2007).
18. Schimel, D. S. Drylands in the Earth system. *Science* **327,** 418–419 (2010).
19. Maestre, F. T. *et al.* It's getting hotter in here: determining and projecting the impacts of global environmental change on drylands. *Phil. Trans. R. Soc. B* **367,** 3062–3075 (2012).
20. Cross, A. F. & Schlesinger, W. H. Biological and geochemical controls on phosphorus fractions in semiarid soils. *Biogeochemistry* **52,** 155–172 (2001).
21. Li, J. *et al.* Quantitative effects of vegetation cover on wind erosion and soil nutrient loss in a desert grassland of southern New Mexico, USA. *Biogeochemistry* **85,** 317–332 (2007).
22. Sinsabaugh, R. L. *et al. Enzymes in the Environment* (Oxford Univ. Press, 2002).
23. Olander, L. P. & Vitousek, P. M. Regulation of soil phosphatase and chitinase activity by N and P availability. *Biogeochemistry* **49,** 175–191 (2000).
24. Schimel, J. P. & Bennett, J. Nitrogen mineralization, challenges of a changing paradigm. *Ecology* **85,** 591–602 (2004).
25. Evans, S. E. & Burke, I. C. carbon and nitrogen decoupling under an 11-year drought in the shortgrass steppe. *Ecosystems (N. Y.)* **16,** 20–33 (2013).

26. Thornton, P. E. *et al.* Influence of carbon–nitrogen cycle coupling on land model response to CO2 fertilization and climate variability. *Glob. Biogeochem. Cycles* **21,** GB4018 (2007).
27. Scheffer, M. *et al.* Early-warning signals for critical transitions. *Nature* **461,** 53–59 (2009).
28. Maestre, F. T. *et al.* Plant species richness and ecosystem multifunctionality in global drylands. *Science* **335,** 214–218 (2012).
29. Hijmans, R. J. *et al.* Very high resolution interpolated climate surfaces for global areas. *Int. J. Clim.* **25,** 1965–1978 (2005).
30. Grace, J. B. *Structural Equation Modelling Natural Systems* (Cambridge Univ. Press, 2006).

Acknowledgements We thank M. Scheffer, N. J. Gotelli and R. Bardgett for comments on previous versions of the manuscript, and all the technicians and colleagues who helped with the field surveys and laboratory analyses. This research is supported by the European Research Council (ERC) under the European Community's Seventh Framework Programme (FP7/2007-2013)/ERC Grant agreement no. 242658 (BIOCOM), and by the Ministry of Science and Innovation of the Spanish Government, grant no. CGL2010-21381. CYTED funded networking activities (EPES, Acción 407AC0323). M.D.-B. was supported by a PhD fellowship from the Pablo de Olavide University.

Author Contributions F.T.M., M.D.-B. and A.G. designed this study. F.T.M. coordinated all field and laboratory operations. Field data were collected by all authors except A.E., A.G., B.G., E.V., M.B. and M.D.W. Laboratory analyses were done by V.O., A.G., M.B., M.D.-B., E.V. and B.G. Data analyses were done by M.D.-B. and M.A.B. The paper was written by M.D.-B., F.T.M., M.D.W. and A.G., and the remaining authors contributed to the subsequent drafts.

Author Information Reprints and permissions information is available at www.nature.com/reprints. The authors declare no competing financial interests. Readers are welcome to comment on the online version of the paper. Correspondence and requests for materials should be addressed to M.D.-B. (mdelbaq@upo.es).

METHODS

Study site and data collection. Field data were collected from 224 dryland sites located in 16 countries from all continents except Antarctica (see ref. 28 for full details on the study sites sampled). Locations for this study were chosen to represent a wide spectrum of abiotic (climatic, soil type, slope) and biotic (type of vegetation, total cover, species richness) features characterizing drylands worldwide. At each site, we established a 30 m × 30 m plot representative of the dominant vegetation. Within each plot, we measured plant cover using the line-intercept method along four 30-m-long transects separated 8 m from each other[28]. Soils were sampled using a stratified random procedure. At each plot, five 50 cm × 50 cm quadrats were randomly placed under the canopy of the dominant perennial plant species and in open areas devoid of perennial vegetation, and a composite sample (0–7.5-cm depth) was obtained from each of them (10–15 soil samples per site were collected; over 2,600 samples were collected and analysed in total). After field collection, soil samples were taken to the laboratory, where they were sieved, air-dried for one month and stored for laboratory analyses. The clay percentage was determined as described in ref. 28.

Selection of soil C, N and P surrogates. The biogeochemical cycles of C, N and P are interlinked with primary production, respiration and decomposition in terrestrial ecosystems[1,12,31]. All these nutrients have a large variety of forms in soils, including different qualities (labile and recalcitrant) and chemistries[12,32,33] (organic and inorganic). Only some of them, however, are available for plants and microorganisms[12,24]. Because of the importance of the biogeochemical cycles of C, N and P on the plant and microorganism stoichiometries[1,3,34], we focused our study on the available nutrient forms for these organisms. Thus, we selected total organic C as our surrogate of the C cycle because we observed that it is a parsimonious summary of labile C sources available to soil microorganisms, as this variable is strongly correlated with the availability of other C sources such as dissolved carbohydrates (Pearson's $r = 0.59$; $P < 0.001$) at the studied sites. Similarly, total N was selected as our N-cycle surrogate because of its relationship to other N forms available for plants and microorganisms, such as dissolved inorganic N (Pearson's $r = 0.40$, $P < 0.001$) and amino acids[12,24,31,33,35] (Pearson's $r = 0.41$, $P < 0.001$). Finally, we selected total P as our P-cycle surrogate because of its relationship to other P forms available for plants and microorganisms[2,13–15,22,36–41]. In our study sites, total P was positively related to available P (Olsen inorganic P; Pearson's $r = 0.43$, $P < 0.001$) and HCl-P (Pearson's $r = 0.23$, $P = 0.001$). The Olsen inorganic P extract (available P) simulates the action of plant roots in dissolving P minerals, and is considered as an index of plant-available P, and the 1 M HCl inorganic P fraction (non-occluded) represents the P associated with calcium carbonate minerals, which is available over long time periods[20,37–39,42,43]. The exchange between P and carbonate minerals limits P availability in desert soils, and the precipitation of phosphate with calcium establishes an upper limit for the availability of P (refs 5,22,42–44).

To avoid problems associated with the use of multiple laboratories when analysing soils from different sites, and to facilitate the comparison of results between them, dried soil samples from all the countries were shipped to Spain for analyses. All the analyses for organic C, Olsen inorganic P, total P and phosphatase activity were carried out at the laboratory of the Biology and Geology Department, Rey Juan Carlos University (Móstoles, Spain). Analyses of total N were carried out at the University of Jaén (Jaén, Spain). The remaining soil analyses were carried out at the laboratory of the Department of Physical, Natural and Natural Systems, Pablo de Olavide University (Sevilla, Spain). Organic C was determined by colorimetry after oxidation with a mixture of potassium dichromate and sulphuric acid[45]. Total N was obtained using a CN analyser (Leco CHN628 Series, Leco Corporation). Total P was measured using a Skalar San++ Analyzer after digestion with sulphuric acid. Olsen inorganic P was measured following a 0.5 M $NaHCO_3$ (pH 8.5) extraction[36,37]. Soil extracts in a ratio of 1:5 were shaken in a reciprocal shaker at 200 r.p.m. for 2 h. An aliquot of the centrifuged extract was used for the colorimetric determination of Olsen inorganic P, on the basis of its reaction with ammonium molybdate[46]; the pH of the extracts was adjusted with 0.1 M HCl when necessary. The 1 M P HCl-P fraction was determined following the soil-P fractionation protocol of ref. 38. The remaining soil variables were measured in K_2SO_4 0.5 M soil extracts in the ratio 1:5. Soil extracts were shaken on an orbital shaker at 200 r.p.m. for 2 h at 20 °C and filtered to pass a 0.45-μm Millipore filter. The filtered extract was kept at 2 °C until colorimetric analyses, which were conducted within 24 h of the extraction. Subsamples of each extract were taken for measurements of carbohydrates (sum of hexoses and pentoses) and amino acids according to ref. 35. Inorganic-N (sum of ammonium and nitrate) concentrations were also measured for each K_2SO_4 0.5 M extract subsample with the indophenol blue method described in ref. 47.

Rationale of the variables included in structural equation modelling. Aridity is a fundamental driver of biological and geochemical processes[5,8,12,48–50] in arid, semi-arid, and dry sub-humid ecosystems (areas where the ratio of precipitation to potential evapotranspiration is less than 0.65 (ref. 28); hereafter drylands), where water availability is the most limiting resource[6–8,17,18]. Aridity determines water availability in drylands, and therefore has a substantial impact on factors such as plant productivity, microbial activity, nutrient concentration and soil enzyme activities[6–8,12,17,18]. This environmental factor has both direct and indirect impacts on ecosystem services, and on multiple processes directly related to ecosystem functioning[5,8]. For example, increasing aridity in drylands has been observed to decrease vegetation cover[43], indirectly promoting soil erosion by wind[3–5,8,17,18,48,51], which can subsequently lead to land degradation and desertification[3–5,8,17,18,48,51]. Wind erosion can remove silt, clay and organic matter from the surface soil, leaving behind sand and infertile materials[51]. In addition, aridity promotes soil drying, increasing its salinity levels and enhancing soil erosion, which effects remove fine, nutrient-rich particles such as clay[3–5,8,17,18,20,43,51].

The cover of perennial vascular plants is also a key driver of ecosystem structure and functioning in drylands, because this variable largely determines processes such as plant facilitation, litter production and decomposition, and biological N fixation, as well as the ability of landscapes to retain water and nutrients[52–58]. Therefore, plant cover is closely related to nutrient availability in dryland soils[12,53–58].

Clay has an important role on the retention of water and nutrients at the soil surface, where microbial activity is greatest, and can also modify local pH[59–63]. The activity of phosphatase was included in our structural equation model because extracellular enzymes are proximate agents of organic matter decomposition and their assessment can be used as an indicator of microbial nutrient demand[15,22]. The activity of extracellular enzymes, which are produced by both plants and microorganisms[15,22], is known to be negatively affected by factors linked to aridity such as low water availability and soil salinity[15,22,64]. Enzyme activities have been observed to be associated with clay abundance in soil[63,64]. Phosphatase is the enzyme responsible for releasing inorganic P from organic sources, and is considered a surrogate of biological P demand[15,22]. Phosphatase activity was measured by determination of the amount of *p*-nitrophenol released from 0.5 g soil after incubation at 37 °C for 1 h with the substrate *p*-nitrophenyl phosphate in MUB buffer (pH 6.5). Inorganic P is a universal source of P for plants and microorganisms[15,20,22,44]. As a component of biological molecules fundamental to cellular energy transfer (that is, ATP and nicotinamide adenine trinucleotide), P has a major role in the C and N fixation in drylands, and is non-biological in origin, being derived from rocks and sediments[1]. Carbon and N are primarily linked to biological processes such as photosynthesis, atmospheric-N fixation and subsequent microbial mineralization[12], and are considered to be key elements for enzyme production[12,14,22,23]. Finally, we included the spatial location (distance from Equator and longitude) of each site in our structural equation model to account for the spatial autocorrelation present in our data (see ref. 28 for a related approach).

Statistical and numerical analyses. Before numerical and statistical analysis, all the variables in this study (plant cover, clay, organic C, total N, total P and activity of phosphatase) were averaged to obtain site-level estimates by using the mean values observed in bare ground and vegetated areas, weighted by their respective cover at each site.

We explored the relationship of aridity with the different selected C (organic C), N (total N) and P (total P) variables, and with the N:P, C:P and N:C ratios, by using either linear or curvilinear (quadratic) regressions. Similarly, we explored the relationship between aridity and inorganic P (sum of Olsen inorganic P and HCl-P), organic C and total N, and that with their respective N:P, C:P and N:C ratios (Extended Data Fig. 1). Among these, the function that minimized the second-order Akaike information criterion[65] was chosen in each case. All the nutrient ratios were log-transformed to achieve normality before conducting these analyses. The aridity index[8,19,51] (AI, the ratio of precipitation to potential evapotranspiration) of each site was calculated using data interpolations provided by WorldClim[29,66]. To facilitate the interpretation of our results, we used $1 - AI$ as our surrogate of aridity. This index increases with decreasing annual mean precipitation in our database ($r = 0.91$, $P < 0.001$). We also explored the relationship of aridity with more labile sources of C (carbohydrates), N (sum of dissolved inorganic N and amino acids) and available P (Olsen inorganic P), as well as with their respective ratios. The results obtained (Extended Data Fig. 2) were very similar to those presented in the main text (Fig. 1); hence, we used total N, organic C and total P there because of their typically high stability in time[67–69].

To determine the relative importance of aridity on the selected soil nutrients differentially linked to biological (C and N) versus geochemical (P) control, we used structural equation modelling[30] (SEM). Overall, SEM has emerged as a synthesis of path analysis, factor analysis and maximum-likelihood techniques, and has been thoroughly used in the ecological sciences as a causal inference tool[30,70]. It can test the plausibility of a causal model, which is based on a-priori information on the relationships among the particular variables of interest. Some data manipulation was required before modelling. We checked the bivariate relationships between all variables to ensure that a linear model was appropriate. We identified

some curvilinear relationships among our variables. Several variables showed a curvilinear relationship with latitude, such that areas closer to the Equator tended to be different from areas farther from the Equator. This was simply handled by expressing latitude as distance from the Equator (that is, the absolute value of latitude). Because longitude has an arbitrary origin, this transformation did not apply to longitude. We found that organic C, total N and the activity of phosphatase were curvilinearly influenced by aridity, and that these relationships were well described by a second-order polynomial. To introduce polynomial relationships into our model, we calculated the square of aridity and introduced it into our model using a composite variable approach described below. We also examined the distributions of all of our endogenous variables, and tested their normality. Organic C, total N, total P and activity of phosphatase were log-transformed to improve normality. Similarly, the plant total cover was square-root-transformed. Because organic C and total N were very closely related (Pearson's $r = 0.92$), we could not introduce them into the same model without risking collinearity. Attempts to construct a latent variable including organic C and total N were not successful. Thus, we reduced these two variables to a single variable using PCA on the correlation matrix, and then introduced this new variable into the model (organic-matter component). We interpret this variable as organic C and N, as both variables were very highly correlated with the PCA component (Pearson's $r = 0.98$); although some of the total N is certainly in mineral form[71], this very close relationship indicates that total N is under tight control of organic matter in the studied drylands. Then, we established an a-priori model (Extended Data Fig. 4) based on the known effects and relationships among the drivers of C, N and P availability. This model accounted for spatial structure (latitude and longitude), aridity, percentage of plant cover and clay, organic matter component (total N and organic C), activity of phosphatase and total P.

When these data manipulations were complete, we parameterized our model using our data set and tested its overall goodness of fit. There is no single universally accepted test of overall goodness of fit for structural equation models, applicable in all situations regardless of sample size or data distribution. Most modellers circumvent this problem by using multiple goodness-of-fit criteria. We used the χ^2-test (the model has a good fit when $0 \leq \chi^2 \leq 2$ and $0.05 < P \leq 1.00$) and the root mean square error of approximation (RMSEA; the model has a good fit when $0 \leq \text{RMSEA} \leq 0.05$ and $0.10 < P \leq 1.00$). Additionally, and because some variables were not normally distributed, we confirmed the fit of the model using the Bollen–Stine bootstrap test[72] (the model has a good fit when $0.10 <$ bootstrap $P \leq 1.00$). Our a-priori model attained an acceptable fit by all criteria, and thus no *post hoc* alterations were made.

After attaining a satisfactory model fit, we introduced composite variables into our model. The use of composite variables does not alter the underlying SEM model, but collapses the effects of multiple conceptually related variables into a single composite effect, aiding interpretation of model results[30,70]. Distance from the Equator and longitude were included as a composite variable, because together they determine the spatial proximity of plots. A separate composite was constructed for each response variable. We also used composite variables to model the nonlinear response to aridity of the organic matter component (first component from a PCA with organic C and total N) and phosphatase activity. As previously mentioned, both aridity and its square are introduced as variables in the model. Because one is mathematically derived from the other, they are allowed to covary. In cases where a nonlinear fit is desired, the effects of aridity and squared aridity on a given response are composited. The resulting effect has no interpretable sign, because the relationship may be positive over some portion of the data and negative over other portions. In cases where a simple linear effect of aridity was desired (for example total P), we simply included a single path from aridity and did not use squared aridity.

With a reasonable model fit, and composite variables constructed, we were free to interpret the path coefficients of the model, and their associated P values. A path coefficient is analogous to a partial correlation coefficient, and describes the strength and sign of the relationships between two variables[30,70]. Because some of the variables introduced were not normally distributed, the probability that a path coefficient differs from zero was tested using bootstrap tests[30,70]. Bootstrapping is preferred to the classical maximum-likelihood estimation in these cases, because in bootstrapping probability assessments are not based on an assumption that the data match a particular theoretical distribution. Thus, data are randomly sampled with replacement to arrive at estimates of standard errors that are empirically associated with the distribution of the data in the sample[30,70].

Another important capability of SEM is its ability to partition direct and indirect effects that one variable may have on another, and estimate the strengths of these multiple effects. Unlike regression or analysis of variance, SEM offers the ability to separate multiple pathways of influence and view them as a system[30,70]. Thus, SEM is useful for investigating the complex networks of relationships found in natural ecosystems[30,70].

To aid final interpretation in light of this ability of SEM, we calculated not only the standardized total effects of aridity, percentage of clay and plant cover, and spatial position (distance from Equator and longitude) on the organic matter component, but also the effect of the organic matter component on phosphatase and total P activity. The net influence that one variable has on another is calculated by summing all direct and indirect pathways between the two variables. If the model fits the data well, the total effect should approximate the bivariate correlation coefficient for that pair of variables[30,70].

In addition, and to support our results further, we repeated our structural equation model including inorganic P (sum of Olsen inorganic P and HCl-P) instead of total P (Extended Data Figs 5 and 6) and using a labile organic matter component (first component from a PCA with carbohydrates and available N) and available P (Olsen inorganic P; Extended Data Figs 7 and 8).

All the SEM analyses were conducted using AMOS 18.0 (Amos Development Co.). The remaining statistical analyses were performed using SPSS 15.0 (SPSS Inc.).

31. Robertson, G. P. & Groffman, P. *Soil Microbiology and Biochemistry* (Springer, 2007).
32. Rovira, P. & Vallejo, V. R. Labile and recalcitrant pools of carbon and nitrogen in organic matter decomposing at different depths in soil: an acid hydrolysis approach. *Geoderma* **107,** 109–141 (2002).
33. Neff, J. C. *et al.* Breaks in the cycle: dissolved organic nitrogen in terrestrial ecosystems. *Front. Ecol. Environ* **1,** 205–211 (2003).
34. Sardans, J. *et al.* The C:N:P stoichiometry of organisms and ecosystems in a changing world: a review and perspectives. *Perspect. Plant Ecol. Evol. Syst.* **14,** 33–47 (2012).
35. Chantigny, M. H. *et al. Soil Sampling and Methods of Analysis* (CRC, 2006).
36. Bray, R. H. & Kurtz, L. T. Determination of total, organic, and available forms of phosphorus in soils. *Soil Sci.* **59,** 39–46 (1945).
37. Olsen, S. R. *et al.* Estimation of available phosphorus in soils by extraction with sodium bicarbonate. *USDA Circ.* **939** (1954).
38. Tiessen, H. & Moir, J. O. *Characterization of Available P by Sequential Fractionation. Soil Sampling and Methods of Analysis* (Lewis, 1993).
39. Carreira, J. A. *et al.* Phosphorus transformations along a soil/vegetation series of fire-prone, dolomitic, semi-arid shrublands of southern Spain. *Biogeochemistry* **39,** 87–120 (1997).
40. Schoenau, J. J. *et al.* Forms and cycling of phosphorus in prairie and boreal forest soils. *Biogeochemistry* **8,** 223–237 (1989).
41. Bowman, R. A. & Cole, C. V. Transformations of organic phosphorus substrates in soils as evaluated by NaHCO3 extractions. *Soil Sci.* **125,** 49–54 (1978).
42. Cross, A. F. & Schlesinger, W. H. A literature review and evaluation of the Hedley fractionation: applications to the biogeochemical cycle of soil phosphorus in natural ecosystems. *Geoderma* **64,** 197–214 (1995).
43. Lajtha, K. & Bloomer, S. H. Factors affecting phosphate sorption and phosphate retention in a desert ecosystem. *Soil Sci.* **146,** 160–167 (1988).
44. Roberts, T. L. *et al.* The influence of topography on the distribution of organic and inorganic soil phosphorus across a narrow environmental gradient. *Can. J. Soil Sci.* **65,** 651–665 (1985).
45. Anderson, J. M. & Ingramm, J. S. I. *Tropical Soil Biology and Fertility: A Handbook of Methods* 2nd edn (CABI, 1993).
46. Tabatabai, M. A. & Bremner, J. M. Use of p-nitrophenyl phosphate for assay of soil phosphatase activity. *Soil Biol. Biochem.* **1,** 301–307 (1969).
47. Delgado-Baquerizo, M. *et al.* A dissolved organic nitrogen in Mediterranean ecosystems. *Pedosphere* **21,** 309–318 (2011).
48. Helmut, G. *The Causes and Progression of Desertification* (Ashgate, 2005).
49. Michael, B. *et al. Human Impact on Environment and Sustainable Development in Africa* (Ashgate, 2003).
50. Johnson, P. J. *Governing Global Desertification: Linking Environmental Degradation, Poverty and Participation* (Ashgate, 2006).
51. Food and Agriculture Organization. *Arid Zone Forestry: A Guide for Field Technicians* Ch. I (Food and Agriculture Organization, 1989).
52. Vitousek, P. M. *et al.* Towards an ecological understanding of biological nitrogen fixation. *Biogeochemistry* **57,** 1–45 (2002).
53. Maestre, F. T. *et al.* Potential of using facilitation by grasses to establish shrubs on a semiarid degraded steppe. *Ecol. Appl.* **11,** 1641–1655 (2001).
54. Reynolds, J. F. *et al.* Impact of drought on desert shrubs: effects of seasonality and degree of resource island development. *Ecol. Monogr.* **69,** 69–106 (1999).
55. Maestre, F. T. *et al.* Positive, negative and net effects in grass-shrub interactions in Mediterranean semiarid grasslands. *Ecology* **84,** 3186–3197 (2003).
56. Eldridge, D. *et al.* Interactive effects of three ecosystem engineers on infiltration in a semi-arid Mediterranean grassland. *Ecosystems (N. Y.)* **13,** 499–510 (2010).
57. Cerdà, A. The effect of patchy distribution of Stipa tenacissima L. on runoff and erosion. *J. Arid Environ.* **36,** 37–51 (1997).
58. Cornelis, W. S. *Dryland Ecohydrology* (Springer, 2006).
59. Blanco, H. & Rattan, R. *Principles of Soil Conservation and Management* (Springer, 2010).
60. Yerima, P. K. *et al. Introduction to Soil Science: Soils of the Tropics* (Trafford, 2005).
61. Marshall, K. C. Clay mineralogy in relation to survival of soil bacteria. *Annu. Rev. Phytopathol.* **13,** 357–373 (1975).
62. Stotzky, G. Activity, ecology, and population dynamics of microorganisms in soil. *Rev. Microbiol.* **2,** 59–137 (1972).
63. Kandeler, E. *Physiological and Biochemical Methods for Studying Soil Biota and Their Function. Soil Microbiology and Biochemistry* (Springer, 2007).

64. Tietjen, T. & Wetzel, R. G. Extracellular enzyme-clay mineral complexes: enzyme adsorption, alteration of enzyme activity, and protection from photodegradation. *Aquat. Ecol.* **37,** 331–339 (2003).
65. Sugiura, N. Further analysis of the data by Akaike's information criterion and the finite corrections. *Commun. Stat. Theor. M.* **A7,** 13–26 (1978).
66. Zomer, R. J. *et al. Carbon, Land and Water: a Global Analysis of the Hydrologic Dimensions of Climate Change Mitigation Through Afforestation/Reforestation.* Research Report 101 (International Water Management Institute, 2006).
67. Schimel, D. S. *et al.* Climatic, edaphic, and biotic controls over storage and turnover of carbon in soils. *Glob. Biogeochem. Cycles* **8,** 279–293 (1994).
68. Schmidt, M. W. I. *et al.* Persistence of soil organic matter as an ecosystem property. *Nature* **478,** 49–56 (2011).
69. Oades, J. M. The retention of organic matter in soils. *Biogeochemistry* **5,** 35–70 (1988).
70. Shipley, B. *Cause and Correlation in Biology: a User's Guide to Path Analysis Structural Equations and Causal Inference* (Cambridge Univ. Press, 2001).
71. Morford, S. L. *et al.* Increased forest ecosystem carbon and nitrogen storage from nitrogen rich bedrock. *Nature* **477,** 78–81 (2011).
72. Schermelleh-Engel. *et al.* Evaluating the fit of structural equation models, tests of significance descriptive goodness-of-fit measures. *Methods Psychol. Res. Online* **8,** 23–74 (2003).

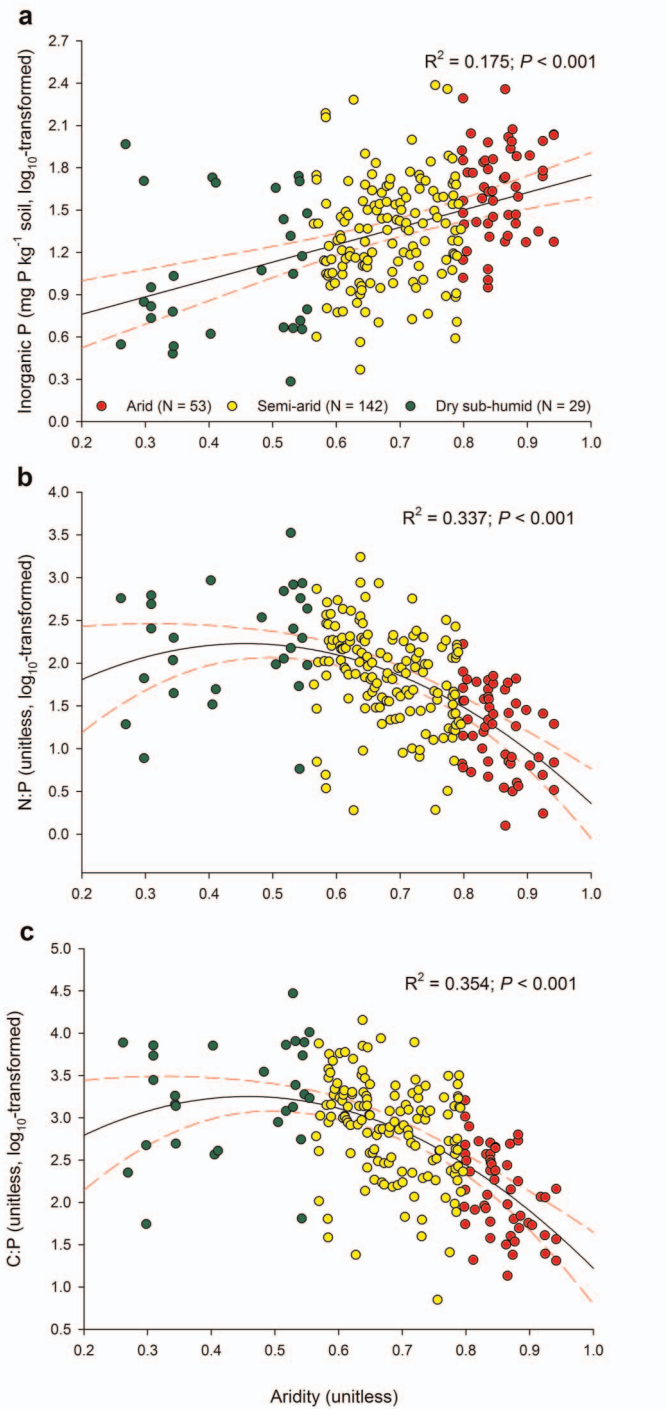

Extended Data Figure 1 | Relationships between aridity and the concentration of inorganic P and the ratios of total N to inorganic P and organic C to inorganic P at our study sites. Inorganic P, sum of Olsen inorganic P and HCl-P. The solid and dashed lines represent the fitted quadratic regressions and their 95% confidence intervals, respectively.

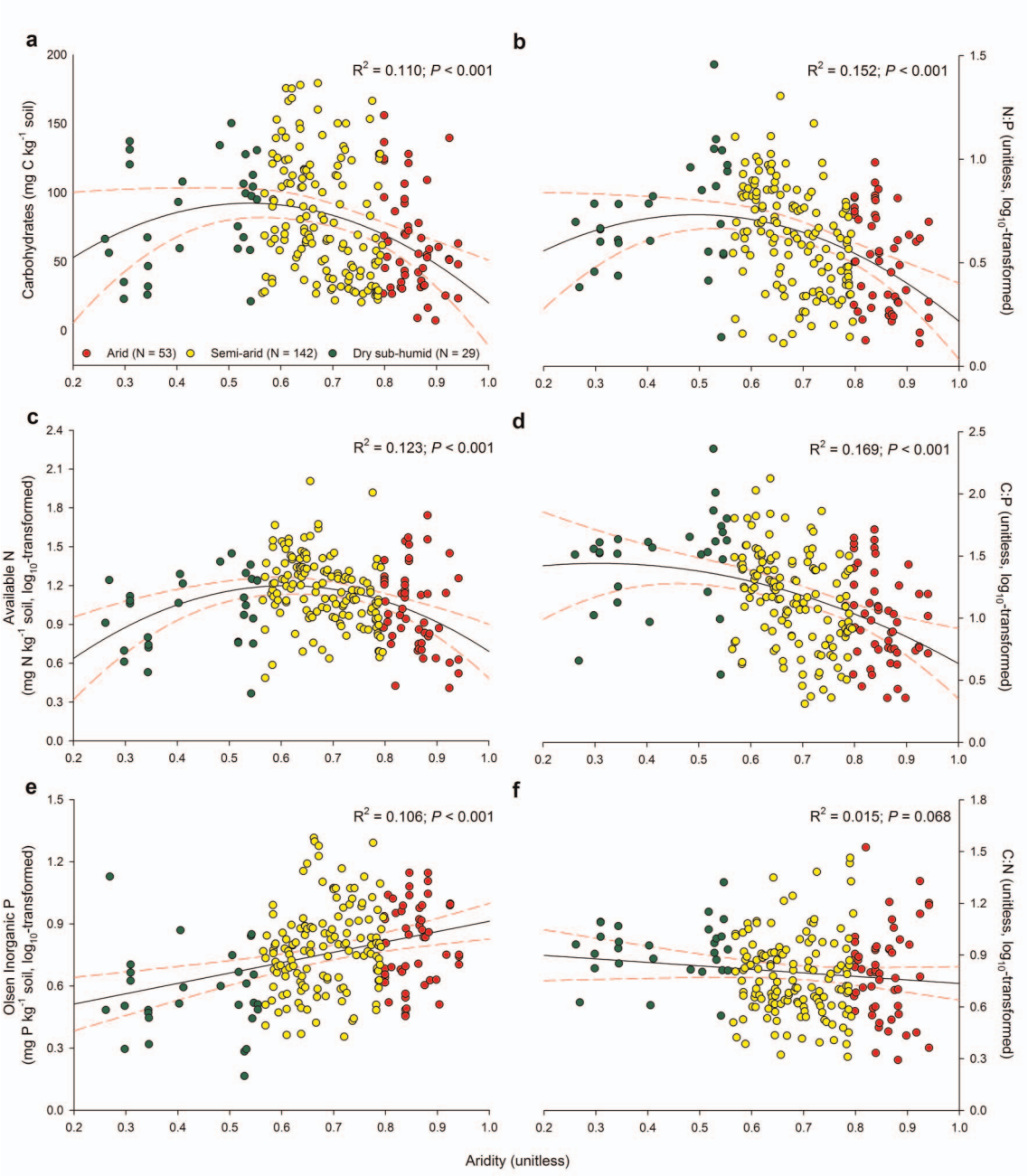

Extended Data Figure 2 | Relationships between aridity and the concentration of carbohydrates (C), available N, available P and their ratios at our study sites. Available N, sum of dissolved inorganic N and amino acids; available P, Olsen inorganic P. The solid and dashed lines represent the fitted quadratic regressions and their 95% confidence intervals, respectively.

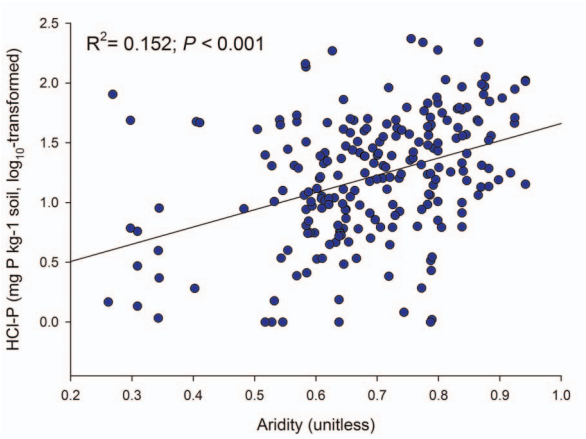

Extended Data Figure 3 | Relationships between aridity and the concentration of HCl-P fraction at our study sites.

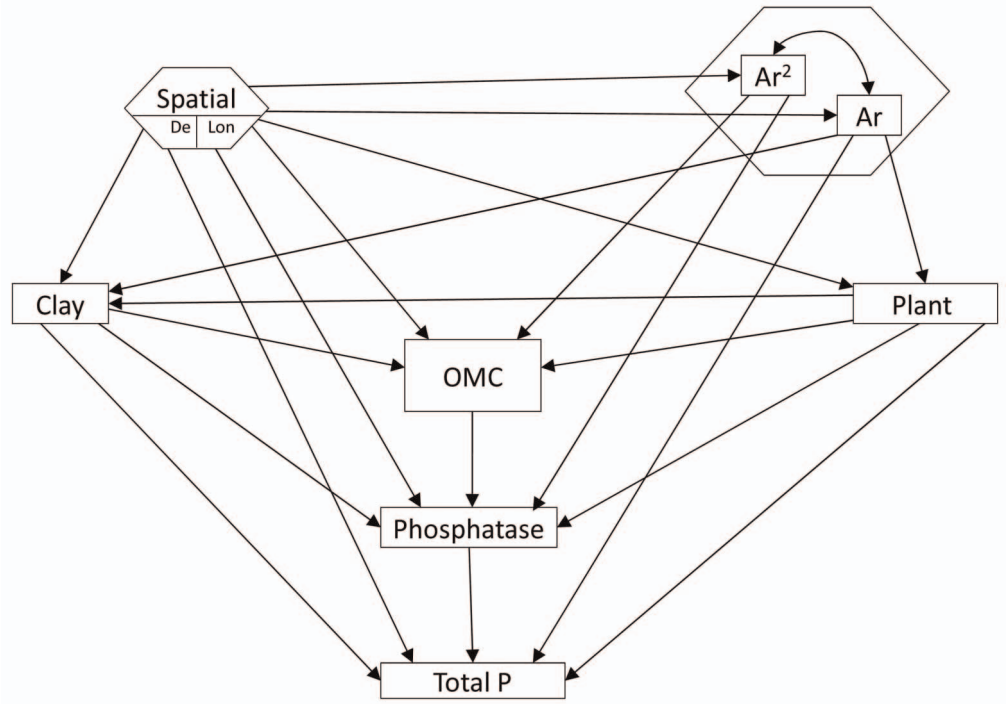

Extended Data Figure 4 | A-priori structural equation model used in this study. We included in this model aridity (Ar; composite variable formed from Ar and Ar^2), percentage of plant cover (Plant), percentage of clay (Clay), spatial position (Spatial; composite variable formed from distance from Equator (De) and longitude (Lon)), activity of phosphatase, organic matter component (OMC; first component from a PCA conducted with organic C (OC) and total N (TN)) and total P. We built our structural equation model by taking into account all these relationship, as explained in Methods. There are some differences between the a-priori model and the final model structures owing to removal of paths with coefficients close to zero (Fig. 2). Hexagons are composite variables[30]. Squares are observable variables.

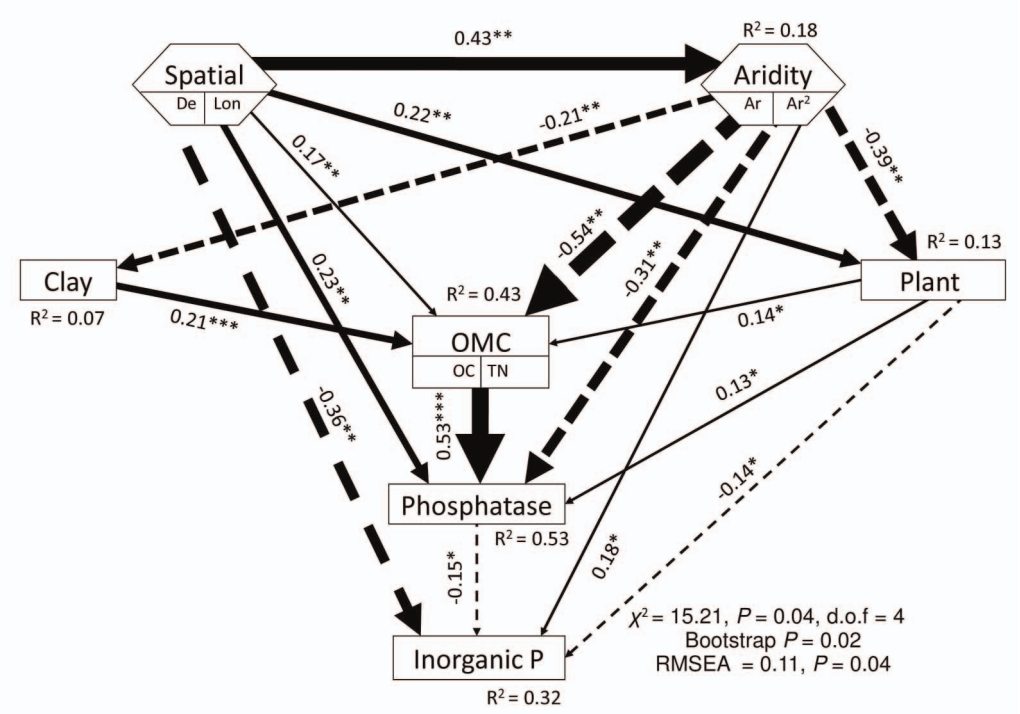

Extended Data Figure 5 | Global structural equation model, depicting the effects of aridity, clay percentage, plant cover and site position on the organic matter component, the inorganic-P concentration and phosphatase activity. Spatial coordinates of the study sites are expressed in terms of distance from Equator (De) and longitude (Lon). The organic matter component (OMC) is the first component from a PCA conducted with organic C and total N. The inorganic-P concentration is the sum of Olsen inorganic P and HCl-P. Numbers adjacent to arrows are standardized path coefficients, analogous to relative regression weights, and indicative of the effect size of the relationship. Continuous and dashed arrows indicate positive and negative relationships, respectively. The width of arrows is proportional to the strength of path coefficients. The proportion of variance explained (R^2) appears above every response variable in the model. Goodness-of-fit statistics for each model are shown in the lower right corner. There are some differences between the a-priori model and the final model structures owing to removal of paths with coefficients close to zero (see the a-priori model in Extended Data Fig. 4). Hexagons are composite variables[30]. Squares are observable variables. $^*P < 0.05$, $^{**}P < 0.01$, $^{***}P < 0.001$.

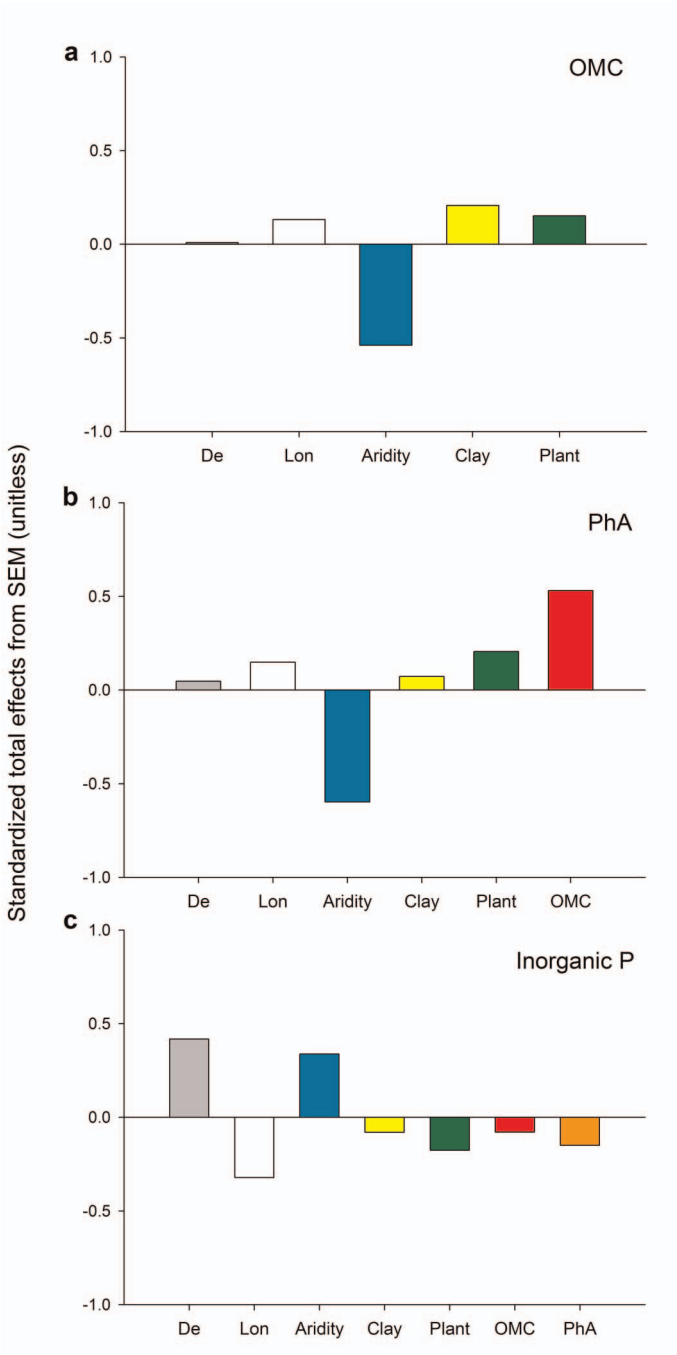

Extended Data Figure 6 | Standardized total effects (direct plus indirect effects) derived from the structural equation modelling. These include the effects of aridity, percentage of clay, plant cover, distance from Equator (De) and longitude (Lon) on the organic matter component (OMC, first component from a PCA conducted with organic C and total N), inorganic P (sum of Olsen inorganic P and HCl-P) and phosphatase activity (PhA).

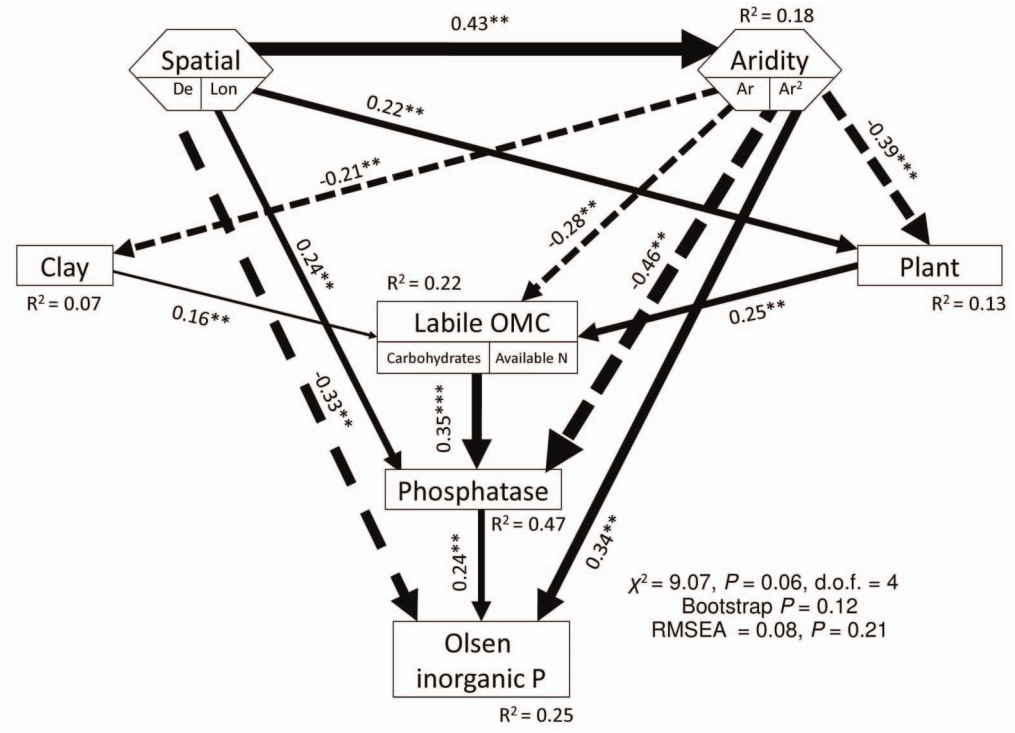

Extended Data Figure 7 | Global structural equation model, depicting the effects of aridity, clay percentage, plant cover and site position on the labile organic matter component, available-P concentration and phosphatase activity. The labile organic matter component (labile OMC) is the first component from a PCA conducted with soil carbohydrates and the ratio of available N to the sum of dissolved inorganic N and amino acids. Available P is the Olsen inorganic P. Numbers adjacent to arrows are standardized path coefficients, analogous to relative regression weights, and indicative of the effect size of the relationship. Continuous and dashed arrows indicate positive and negative relationships, respectively. The width of arrows is proportional to the strength of path coefficients. The proportion of variance explained (R^2) appears above every response variable in the model. Goodness-of-fit statistics for each model are shown in the lower right corner. There are some differences between the a-priori model and the final model structures owing to removal of paths with coefficients close to zero (see the a-priori model in Extended Data Fig. 4). Hexagons are composite variables[30]. Squares are observable variables. $^*P < 0.05$, $^{**}P < 0.01$, $^{***}P < 0.001$.

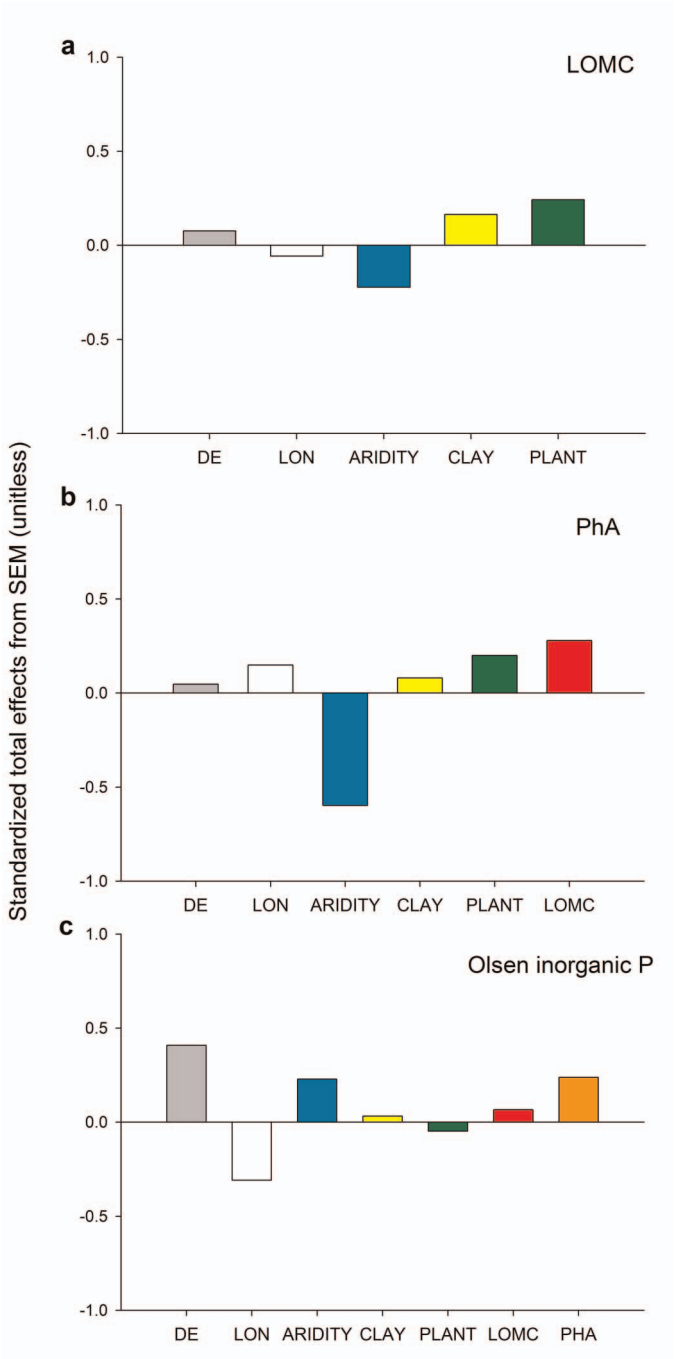

Extended Data Figure 8 | Standardized total effects (direct plus indirect effects) derived from the structural equation modelling. These include the effects of aridity, percentage of clay, plant cover, distance from Equator (De) and longitude (Lon) on the labile organic matter component (LOMC, first component from a PCA conducted with carbohydrates and available N), available P (Olsen inorganic P) and phosphatase activity (PhA).

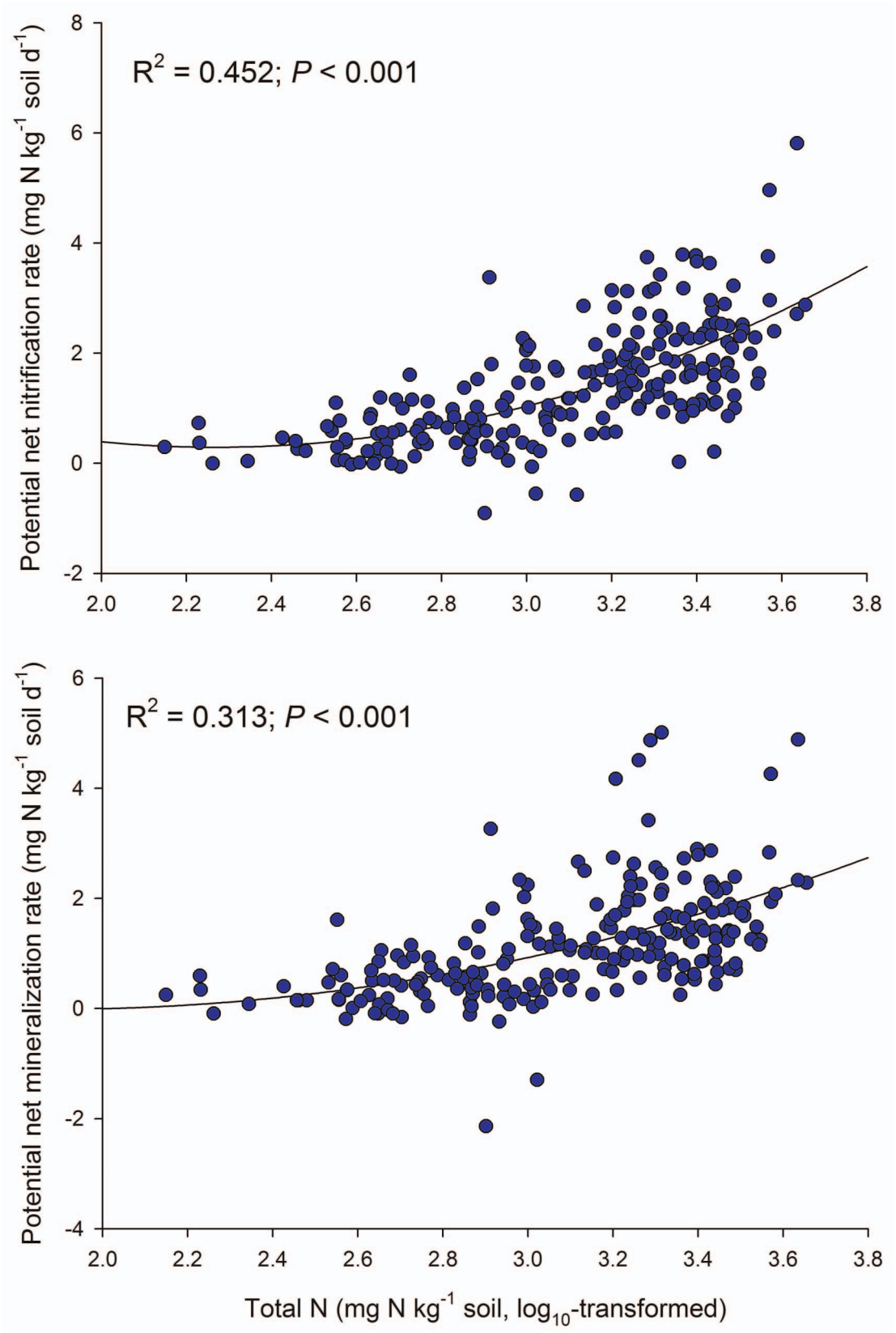

Extended Data Figure 9 | Relationships between total N and the potential net nitrification (upper graph) and mineralization rates (lower graph) measured at our study sites. Air-dried soil samples were re-wetted to reach 80% of field water-holding capacity and incubated in the laboratory for 14 days at 30 °C (ref. 28). Potential net nitrification and ammonification rates were estimated as the difference between initial and final nitrate and ammonium concentrations[28]. The solid line denotes the quadratic model fitted to the data (R^2 and P values shown in each panel).

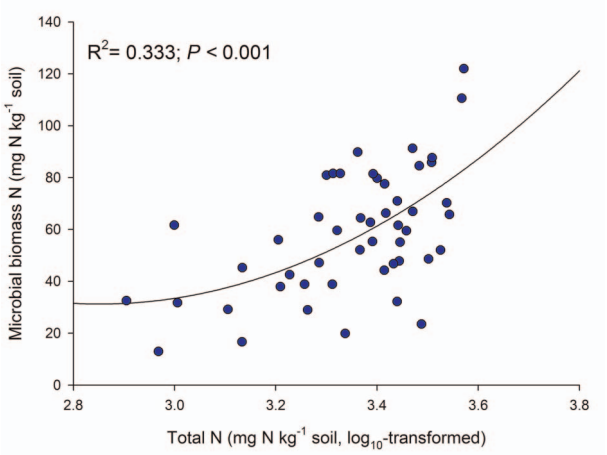

Extended Data Figure 10 | Relationships between the total N and microbial biomass N in a subset of 50 of our 224 sites. All air-dried soil samples were adjusted to 55% of their water-holding capacity previous to the analyses of microbial biomass N. Microbial biomass N was determined using the fumigation–extraction method. Non-incubated and incubated soil subsamples were fumigated with chloroform for five days. Non-fumigated replicates were used as controls. Fumigated and non-fumigated samples were extracted with K_2SO_4 0.5 M in the ratio 1:5 and filtered through a 0.45-μm Millipore filter. Concentration of microbial biomass N was estimated as the difference between total N of fumigated and non-fumigated digested extracts[28] and then divided by 0.54 (that is, by Kn, the fraction of biomass N extracted after the CHC_{13} treatment). The solid line denotes the quadratic model fitted to the data (R^2 and P values shown in the graph).